

Temporal and structural heterogeneities emerging in adaptive temporal networks

Takaaki Aoki,^{1,*} Luis E. C. Rocha,^{2,3} and Thilo Gross⁴

¹*Faculty of Education, Kagawa University, Takamatsu, Japan*

²*Department of Mathematics, Université de Namur, Namur, Belgium*

³*Department of Public Health Sciences, Karolinska Institutet, Stockholm, Sweden*

⁴*Department of Engineering Mathematics, University of Bristol, Bristol, UK*

(Dated: October 2, 2015)

We introduce a model of adaptive temporal networks whose evolution is regulated by an interplay between node activity and dynamic exchange of information through links. We study the model by using a master equation approach. Starting from a homogeneous initial configuration, we show that temporal and structural heterogeneities, characteristic of real-world networks, spontaneously emerge. This theoretically tractable model thus contributes to the understanding of the dynamics of human activity and interaction networks.

PACS numbers: 05.65.+b, 89.75.Fb, 89.75.Hc

Human social behaviour depends both on intrinsic properties of the individuals and on the interactions between them. In daily life, interactions between people create contact patterns that can be mathematically represented by networks, i.e. a set of nodes, corresponding to the people, connected by links, representing the contacts between the respective individuals [1]. In network terminology, the number of contacts of a given person is called the degree k of a node and thus the degree distribution p_k is the probability distribution that a randomly chosen node has degree k . A central observation is that real-life networks have a high level of heterogeneity in the number of contacts per node and the empirical degree distributions are typically approximated by power-laws $p_k \sim k^{-\gamma}$ [2–4].

A second observation is that human contact networks are not static. For instance in studies of email contact networks, users that are hubs of the network in one time window may be unremarkable or even isolated in the next time window [5]. Recent studies suggest that this is due to a change in the intrinsic state of the node between an active, contact-seeking state, and an inactive state. The temporal heterogeneity can then be quantified in terms of the inter-event intervals (IETs) between node activations, which reveals burstiness of human behavior [6–8].

While several models have been proposed to explain the heterogeneity in the degree distribution [9–12], fewer studies focused on modeling the burstiness of the temporal activity [6, 7, 13]. Barabási proposed a priority-based model in which nodes first execute the high-priority tasks, i.e. these tasks are executed within a short time, while low-priority tasks have to wait longer times before leaving the queue. Other models use inhomogeneous Poisson processes on each node modulated by (daily and weekly) cycles of human activity [14, 15]. Combined, these processes generate the patterns of burstiness that are comparable to real world data.

While previous models thus describe network heterogeneity and burstiness as different phenomena, they are connected in the real world: Network structure is a result of the activity of the network nodes, while changes

in activity are likely to be triggered by neighbours in the network. The system is thus be modelled as an adaptive network [16, 17], where dynamics of nodes is thus affected by network structure, while the evolution of the structure is dependent on the state of the nodes.

In this letter, we propose a model of temporal networks where the human activity and their connections are adaptively regulated by past interactions, as illustrated in Fig. 1(a). We analyze the master equation of the model using generating functions. We show that, starting from homogeneous initial conditions, structural heterogeneity and temporal burstiness can emerge spontaneously.

We consider a population of N nodes, where each node i has an intrinsic variable x_i , which we interpret as an abstract resource representing the nodes willingness to engage with others in the network. Initially every node is assigned the same resource quantity, i.e., $x_i(0) = 1$. The system then evolves due to dynamical updates which comprise three steps: (i) activation of nodes, (ii) formation of pairs, and (iii) exchange of resources (Fig. 1(b)).

In the activation step (i) N_A nodes are set to the active state, while all others are set to the inactive state. The active nodes are chosen using a linear preferential rule, such that the probability that node i becomes active scales with x_i . In the pair formation step (ii) every active node picks a partner. With probability κ this partner is chosen randomly from all nodes in the system. With the complementary probability $1 - \kappa$ the partner is chosen randomly from the set of active nodes. This reduces to previously studied rules in the limit $\kappa = 0$ [18], where partners are only picked among the active nodes, and in the limit $\kappa = 1$ [19], where partners are picked among the whole network. Finally, in the exchange step nodes transfer an amount of resource to their partners such that

$$x_i(t+1) - x_i(t) = D \left[\sum_j a_{ij}(t) - \sum_j a_{ji}(t) \right], \quad (1)$$

where D is the amount of resource transferred in the interaction, and $a_{ij}(t) = 1$ is if i has picked j as its

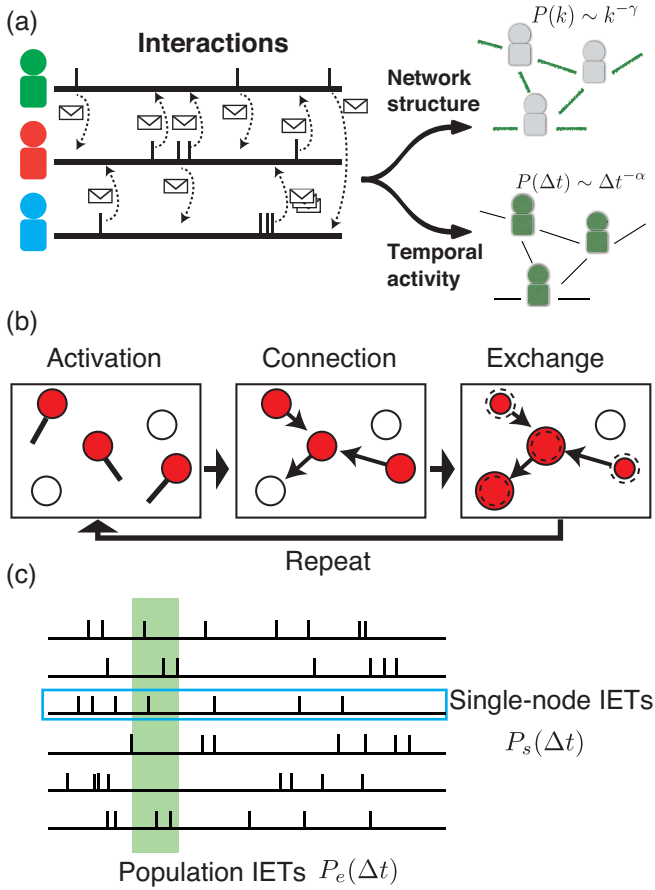


FIG. 1: (a) Question : How do social interactions induce structural and temporal heterogeneities among people? (b) Illustration of the interaction-regulated stochastic contact model. Within one time step, (i) nodes become activate, (ii) make random connections, (iii) exchange resources, and finally (iv) break down the links. (c) Two types of inter-event intervals (IETs): single-node and population.

partner, and 0 otherwise.

In the following we consider the model from a network perspectives. Node i picking a partner j constitutes the creation of a directed link from i to j . Thus the matrix \mathbf{a} is interpreted as a directed adjacency matrix.

To make theoretical progress we construct a master equation for the resource dynamics. We define $u_n(t)$ as the density of nodes i at resource level $x_i = nD$. Setting the total resource in the system to $\sum nDu_n = 1$ and assuming large N and N_A , the probability that a node at resource level n becomes active is $a_n = (N_A/N)(nD/\sum_n nDu_n) = nDN_A/N$. Therefore, the proportion of nodes that are both active and at resource level n is $a_n u_n = N_A n D u_n / N$.

Since the total number of active nodes is N_A , N_A links are formed in every time step. Of these $M_1 := N_A \kappa$ links point to random targets chosen among the whole population, whereas $M_2 := N_A(1 - \kappa)$ point to targets chosen only among the active nodes. From the perspective of

a single node the placement of a link can be seen as a statistical trial that is successful if that specific node is chosen as the target of the link. Every node, irrespective of state, receives a link with probability $\rho_1 = 1/N$ in each of the M_1 trials where the targets are random nodes. In addition, active nodes receive a link with probability $\rho_2 = 1/N_A$ in each of the M_2 trials where the targets are random active nodes.

Each node then gains D units of resource for every incoming link, while active nodes lose D units of resource via their outgoing link. Using the Binomial distribution $B(m, \rho, M)$ of m success in M trials, then leads to the master equation

$$\begin{aligned} \frac{du_n}{dt} = & A(-1)a_{n+1}u_{n+1} \\ & - C_1 a_n u_n - C_2 \bar{a}_n u_n \\ & + \sum_{m=1}^{N_A} a_{n-m} u_{n-m} A(m) \\ & + \sum_{m=1}^{N_A \kappa} \bar{a}_{n-m} u_{n-m} B(m, \rho_1, M_1), \end{aligned} \quad (2)$$

where we now treat time continuously and $\bar{a}_n (= 1 - a_n)$ is the inactive fraction of $u_n(t)$, $A(m) = \sum_{m_1+m_2=m+1} B(m_1, \rho_1, M_1)B(m_2, \rho_2, M_2)$, and $C_1 = 1 - A(0)$, $C_2 = \sum_{m=1}^{N_A \kappa} B(m, \rho_1, N_A \kappa)$.

For the analysis of the master equation it is useful to write a generating function $Q(t, x) = \sum_n u_n(t)x^n$ [20] [22]. This function encodes the u_n in a continuous function by interpreting them as Taylor coefficients in an abstract variable x , which does not have a physical meaning. Multiplying equation (2) by x^n and summing over $n \geq 0$ we obtain

$$\begin{aligned} \frac{\partial Q}{\partial t} = & \frac{N_A D}{N} \frac{\partial Q}{\partial x} \left[A(-1) + (-C_1 + C_2)x + \sum_{m=1}^{N_A-1} A(m)x^{m+1} \right. \\ & \left. - \sum_{m=1}^{N_A \kappa} B(m, \rho_1, M_1)x^{m+1} \right] \\ & + Q \left[-C_2 + \sum_{m=1}^{N_A \kappa} B(m, \rho_1, M_1)x^m \right]. \end{aligned} \quad (3)$$

In the limit $N, N_A \rightarrow \infty$, we approximate the Binomial distributions reduce to Poisson distributions with finite rates, $\lambda_1 (= \rho_1 M_1 = \frac{N_A}{N} \kappa)$ and $\lambda_2 (= \rho_2 M_2 = 1 - \kappa)$, respectively. We obtain

$$\frac{\partial Q}{\partial t} = \frac{N_A D}{N} Y(x) \frac{\partial Q}{\partial x} + Z(x)Q, \quad (4)$$

where $Y(x) = \exp((\lambda_1 + \lambda_2)(x - 1)) - x \exp(\lambda_1(x - 1))$ and $Z(x) = -1 + \exp(\lambda_1(x - 1))$. Thus the generating approach has converted the large system of ordinary differential equations to a single partial differential equation.

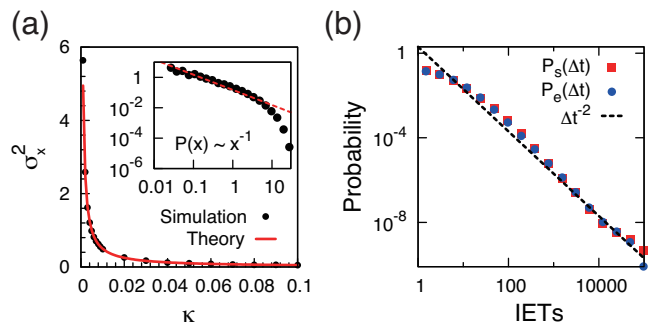


FIG. 2: (a) The variance σ_x^2 of the stationary resource distribution given by Eq. (A4) (red line) and for the simulation of the agent-based model (black circles). We use $D = 0.01$, $N_A = 1000$, and $N = 2^{15}$. The inset shows the resource distribution for $\kappa = 0.001$. (b) The distributions of population and single-node IETs, respectively $P_e(\Delta t)$ and $P_s(\Delta t)$. The master equation analysis predicts $P_e(\Delta t) \propto \Delta t^{-2}$.

When considered in the stationary state, Eq. (4) relates Q to its own first derivative Q' . For any probability distribution the corresponding generating function must obey $Q(1) = 1$. We can therefore find $Q'(1)$ and by differentiating $Q''(1)$. These quantities are of interest because $Q'(1) = \mu$ is the mean of u_n and $Q''(1)$ is closely related to the variance $\sigma^2 = Q''(1) + Q'(1) - Q'(1)^2$ of u_n . From this we can obtain the mean μ_x and variance σ_x^2 of the resource distribution

$$\mu_x = 1, \quad (5)$$

$$\sigma_x^2 = \frac{D}{2\kappa} \left[1 - 2\kappa + \left(1 - \frac{N_A}{N} \right) \kappa^2 \right] + D. \quad (6)$$

In the case where targets are almost always chosen among the active nodes ($\kappa \sim 0$), we find the resource amounts among nodes will be extremely heterogeneous. This result is also found in agent based simulations as shown in the inset of Fig. 2(a), in which the resource distribution is well fitted by a power-law x^{-1} in some ranges. We further confirmed that the same scaling behaviour also appears in a continuous-time version of the model (not shown). These results are interesting since the power law exponent $\gamma = 1$ differs from the $2 < \gamma < 3$ that one would typically expect. At present we do not have an explanation for this exponent and cannot strictly exclude that the $1/k$ behaviour is an extremely long transient.

The master equation loses information on the temporal activity of the nodes. Instead of single-node IETs $P_s(\Delta t)$, we thus consider the population IETs $P_e(\Delta t)$ (Fig. 1(c)). If the amount of resources is fixed, the activation of u_n^* can be described by a Poisson process with a fixed rate a_n . In general, the population IETs of homogeneous Poisson nodes $\{p_i\}$ ($i = 1, 2, \dots, N$) is given

by [15]

$$P_e(\Delta t) = \sum_i p_i e^{-p\Delta t} = \int f(p) p e^{-p\Delta t} dp,$$

where $f(p)$ is the rate distribution in the limit of $N \rightarrow \infty$. In this equation, only the first time-interval of the node's activations is collected for each node [15]. The second, third and succeeding intervals should be taken into account for population IETs during a given observation period. The higher the rate of a node, the more likely the IET data is collected from this node. The probability of the IET should be multiplied by the rate p , and then the equation is rewritten as

$$P_e(\Delta t) = \int f(p) p^2 e^{-p\Delta t} dp \propto \Delta t^{-2}. \quad (7)$$

In the last part, we considered the case of $f(p) \propto p^{-1}$, because u_n^* follows the power-law with exponent -1 . Figure 2(b) shows the distributions of the population IETs with the observation period $T_o = 10^5$ and of the single-node IETs of a uniformly sampled node, obtained by the direct simulation of the model with the same parameters as in Fig. 2(a). We find that both IETs, $P_e(\Delta t)$ and $P_s(\Delta t)$, are close to the power-law predicted theoretically.

By tuning the parameter κ , this model is able to reproduce different structural and temporal patterns (Fig. 3). If $\kappa = 0$, a small group of active nodes emerges. Nodes outside this group are left without resources. In this situation, the diameter of the aggregated contact network (formed by all links collected during $T_s = 10^4$ time steps) shrinks and the temporal patterns of the nodes inside this group exhibit a Poisson-like dynamics, i.e. exponential inter-event times (Fig. 3(b)). By contrast, sufficiently large κ leads to a homogeneous distribution of resources, which generates a Gaussian-like in-degree distribution (Fig. 3(e)) and an exponential (single-node) IET distribution (Fig. 3(f)), the later a result of the quasi-homogenous Poisson process.

In the intermediate case, where active nodes mainly link to other active individuals but also occasionally inactive ones, we observe the emergence of highly heterogeneous structure (Fig. 3(c)) and temporal patterns (Fig. 3(d)). This is the same condition in which we have analytically obtained the power-law distributions of resources and IETs (Fig. 2). The contact network has a power-law in-degree distribution with an exponential cutoff, similar to the resource distribution (Fig. 3(c)). More generally, Figures 3(g) and (h) show the range of the parameters where the model generates either power-law or exponential distribution of IETs. In particular, we see that the range of values of κ , where the heterogeneous structural and temporal patterns emerge (colored circles), is broader for larger values of N_A and D . Note that there is discontinuity between $\kappa = 0$ and $\kappa = \epsilon (> 0)$. If the resource exchange only occurs between active nodes ($\kappa = 0$), all of the resource is occupied by a few nodes, and the heterogeneous temporal behavior does

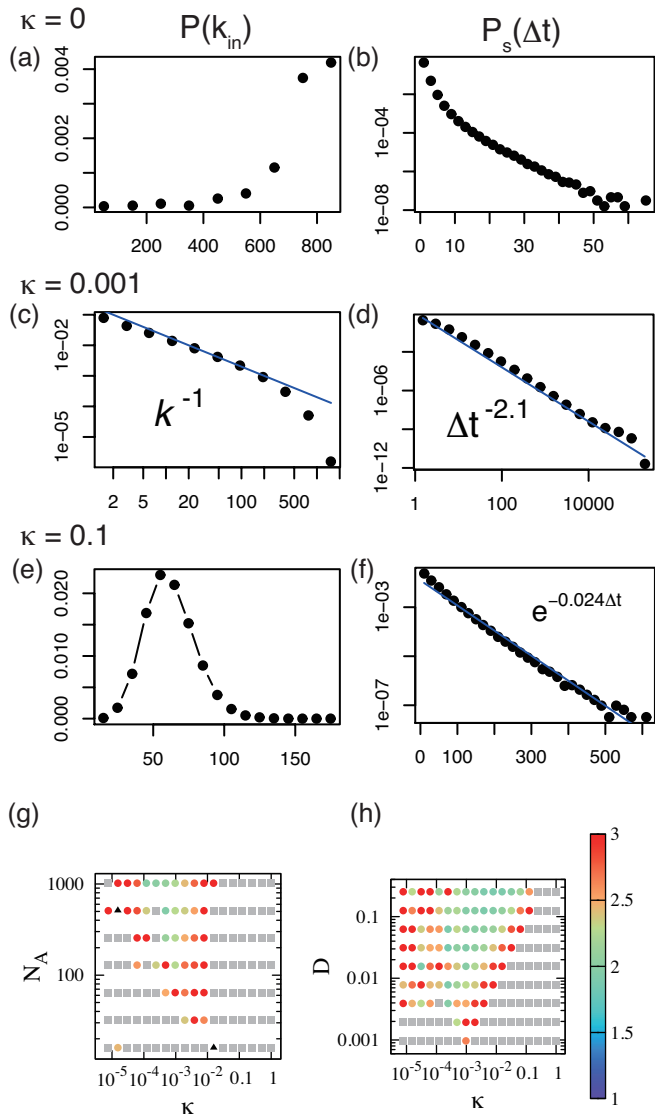


FIG. 3: The degree distribution $P(k)$ and single-node IETs distribution $P_s(\Delta t)$ for (a,b) $\kappa = 0$ ($P_s(\Delta t)$ is plotted in semi-log graph), (c,d) $\kappa = 0.001$ (both graphs are log-log), and (e,f) $\kappa = 0.1$ ($P_s(\Delta t)$ is semi-log), with $N_A = 1024$, $N = 2^{15}$, and $D = 0.01$. Parameter dependency of the model on (g) (κ, N_A) with $D = 0.01$ and (h) (κ, D) with $N_A = 1024$ (log-log graphs). Circles indicate that $P_s(\Delta t)$ follows a power-law distribution, and colors indicate the power-law exponent. Squares indicate an exponential IETs distribution. Black triangles mean that both distributions failed the Vuong's fitting test [21] for that combination of parameters.

not emerge. Our results suggest that an occasional exchange to inactive nodes plays an important role for the emergence of the temporal and structural heterogeneities.

In this paper, we proposed a model of contact networks where the human dynamics are adaptively regulated by past interaction and exchange of resources. We analyzed the master equation of the model and found structural and temporal heterogeneities. This revealed that, the two types of heterogeneity can be observed in rich-club-like systems where the active individuals typically communicate with other active individuals, but occasionally connect to anyone in the network. In these networks spatial and temporal heterogeneity, closely reminiscent of observations in real-world temporal networks, can spontaneously emerge.

This model is perhaps too simplified to realistically represent real-world contact networks. It neglects, for example, the memory effect of friendship relations in contact networks. It also misses the cycles of human activity. These limitations are possibly responsible for the mismatch, in the power-law exponents, of our model and some real-world networks, as for example cell-phone communication shows exponents of the IETs distribution of about 1 [6, 7] and the exponent of degree distribution ranges from 2 to 3.

Nevertheless, the model, despite its simplicity points to a number of unsolved questions, including the exact nature of the observed transition. We therefore hope that it will stimulate future work, leading to deeper insights in the behavioral patterns of humans.

We thank T. Takaguchi, N. Perra, N. Masuda, and S. Shinomoto for fruitful discussions. This work was supported by JSPS KAKENHI Grants No. 24740266 and No. 26520206 and by Bilateral Joint Research Projects between JSPS and F.R.S.-FNRS. LECR is a FNRS Chargé de recherche and thanks Hierta-Retzius Foundation for financial support.

* Electronic address: takaaki.aoki.work@gmail.com

- [1] M. Newman, *Networks: An Introduction* (Oxford University Press, Inc., New York, NY, USA, 2010).
- [2] R. Albert and A. Barabasi, *Rev. Mod. Phys.* **74**, 47 (2002).
- [3] M. Newman, *SIAM Review* **45**, 167 (2003).

- [4] J. Ugander, B. Karrer, L. Backstrom, and C. Marlow, arXiv:1111.4503.
- [5] S. A. Hill and D. Braha, *Phys. Rev. E* **82**, 046105 (2010).
- [6] A.-L. Barabasi, *Nature* **435**, 207 (2005).
- [7] A. Vázquez, J. G. Oliveira, Z. Dezsö, K.-I. Goh, I. Kondor, and A.-L. Barabási, *Phys. Rev. E* **73**, 036127 (2006).

- [8] P. Holme and J. Saramäki, *Physics Reports* **519**, 97 (2012).
- [9] A. Barabási and R. Albert, *Science* **286**, 509 (1999).
- [10] G. Caldarelli, A. Capocci, P. De Los Rios, and M. A. Muñoz, *Phys. Rev. Lett.* **89**, 258702 (2002).
- [11] F. Papadopoulos, M. Kitsak, M. A. Serrano, M. Boguna, and D. Krioukov, *Nature* **489**, 537 (2012).
- [12] L. Muchnik, S. Pei, L. C. Parra, S. D. S. Reis, J. S. Andrade Jr, S. Havlin, and H. A. Makse, *Sci. Rep.* **3**, 1783 (2013).
- [13] S. Vajna, B. Tóth, and J. Kertész, *New Journal of Physics* **15**, 103023 (2013).
- [14] R. D. Malmgren, D. B. Stouffer, A. E. Motter, and L. A. N. Amaral, *Proc. Natl Proc. Acad. Sci. USA* **105**, 18153 (2008).
- [15] C. A. Hidalgo R., *Physica A: Statistical Mechanics and its Applications* **369**, 877 (2006).
- [16] H. Sayama, I. Pestov, J. Schmidt, B. J. Bush, C. Wong, J. Yamanoi, and T. Gross, *Computers & Mathematics with Applications* **65**, 1645 (2013).
- [17] T. Gross and B. Blasius, *J. R. Soc. Interface* **5**, 259 (2008).
- [18] L. E. C. Rocha, F. Liljeros, and P. Holme, *PLoS Computational Biology* **7**, e1001109 (2011).
- [19] N. Perra, B. Gonçalves, R. Pastor-Satorras, and A. Vespignani, *Scientific Reports* **2**, 469 (2012).
- [20] H. S. Wilf, *Generatingfunctionology* (A. K. Peters, Ltd., Natick, MA, USA, 2006).
- [21] Q. H. Vuong, *Econometrica* **57**, 307 (1989).
- [22] See appendix for details on the generating function

Appendix A: Solution of the master equation using generating functions

In this supplementary material we present a detailed derivation of the solution of equation (2) presented in the main text. The equation (2) can be expressed as follows:

$$\frac{du_n(t)}{dt} = A(-1)a_{n+1}u_{n+1}(t) - C_1a_nu_n(t) - C_2\bar{a}_nu_n(t) + \sum_{m=1}^{N_A} a_{n-m}u_{n-m}(t)A(m) + \sum_{m=1}^{N_A\kappa} \bar{a}_{n-m}u_{n-m}(t)B_1(m),$$

where $a_n = \frac{N_A}{N}Dn$, $\bar{a}_n = 1 - a_n$, $B_1(m) = B(m, \rho_1, M_1)$, $B_2(m) = B(m, \rho_2, M_2)$, $A(m) = \sum_{m_1+m_2=m+1} B_1(m_1)B(m_2)$, and $C_1 = 1 - A(0)$, $C_2 = 1 - B_1(0)$.

To solve the master equation above, we define a generating function $Q(t, x) = \sum_n u_n(t)x^n$. Multiplying the master equation above by x^n and summing over $n \geq 0$, we obtain:

$$\begin{aligned} \frac{\partial Q}{\partial t} = & \eta \frac{\partial Q}{\partial x} \left[A(-1) + (-C_1 + C_2)x + \sum_{m=1}^{N_A-1} A(m)x^{m+1} - \sum_{m=1}^{N_A\kappa} B(m, \rho_1, M_1)x^{m+1} \right] \\ & + Q \left[-C_2 + \sum_{m=1}^{N_A\kappa} B(m, \rho_1, M_1)x^m \right], \end{aligned} \quad (\text{A1})$$

where $\eta = \frac{N_A D}{N}$. We used the following relations:

$$\begin{aligned}
\frac{\partial Q}{\partial t} &= \sum_{n \geq 0} \frac{du_n(t)}{dt} x^n \\
\sum_{n \geq 0} a_n u_n(t) x^n &= \eta \sum_{n \geq 0} n u_n(t) x^n = \eta x \frac{\partial Q}{\partial x} \\
\sum_{n \geq 0} a_{n+1} u_{n+1}(t) x^n &= \eta \sum_{n=0}^{\infty} (n+1) u_{n+1}(t) x^n = \eta \left[\sum_{n=1}^{\infty} n u_n(t) x^{n-1} - (n u_n(t) x^n)|_{n=0} \right] \\
&= \eta \frac{\partial Q}{\partial x} \\
\sum_{n \geq 0} a_{n-m} u_{n-m}(t) x^n &= \eta \sum_{n=0}^{\infty} (n-m) u_{n-m}(t) x^n = \eta \sum_{n=0}^{\infty} (n-m) u_{n-m}(t) x^{n-m-1} \cdot x^{m+1} \\
&= \eta x^{m+1} \frac{\partial Q}{\partial x} \\
\sum_{n \geq 0} \bar{a}_n u_n(t) x^n &= \sum_{n \geq 0} (1 - \eta n) u_n(t) x^n = \sum_{n \geq 0} u_n(t) x^n - \eta \sum_{n \geq 0} n u_n(t) x^n \\
&= Q - \eta x \frac{\partial Q}{\partial x} \\
\sum_{n \geq 0} \bar{a}_{n-m} u_{n-m}(t) x^n &= \sum_{n \geq 0} (1 - \eta(n-m)) u_{n-m}(t) x^n = \sum_{n \geq 0} u_{n-m}(t) x^n - \eta \sum_{n \geq 0} (n-m) u_{n-m}(t) x^n \\
&= x^m \sum_{n \geq 0} u_{n-m}(t) x^{n-m} - \eta x^{m+1} \sum_{n \geq 0} (n-m) u_{n-m}(t) x^{n-m-1} \\
&= x^m Q - \eta x^{m+1} \frac{\partial Q}{\partial x}
\end{aligned}$$

In the limit that $\rho \rightarrow 0$ and $M \rightarrow \infty$ with a finite ρM , the Binomial probability can be approximated by the Poisson distribution:

$$B(m, \rho, M) \sim \frac{\lambda^m e^{-\lambda}}{m!},$$

where $\lambda = \rho M$. We now consider the limit, $N, N_A \rightarrow \infty$, with finite ratios $\rho_1 M_1 = \frac{N_A}{N} \kappa$ ($\equiv \lambda_1$), $\rho_2 M_2 = 1 - \kappa$ ($\equiv \lambda_2$).

The terms in the equation (A1) can be rewritten as:

$$\sum_{m=1}^{N_A \kappa} B_1(m)x^m \sim \sum_{m=1}^{N_A \kappa} \frac{(\lambda_1 x)^m e^{-\lambda_1}}{m!} \rightarrow e^{-\lambda_1}[-1 + e^{\lambda_1 x}] \quad (N_A \rightarrow \infty)$$

$$\sum_{m=1}^{N_A \kappa} B_1(m)x^{m+1} \rightarrow x e^{-\lambda_1}[-1 + e^{\lambda_1 x}]$$

$$C_1 = 1 - \sum_{m_1+m_2=1} B_1(m_1)B_2(m_2) = 1 - [B_1(0)B_2(1) + B_1(1)B_2(0)] \\ \sim 1 - [\lambda_1 \cdot e^{-\lambda_1} e^{-\lambda_2} + e^{-\lambda_1} \cdot \lambda_2 e^{-\lambda_2}] = 1 - e^{-(\lambda_1+\lambda_2)}(\lambda_1 + \lambda_2)$$

$$C_2 = 1 - B_1(0) \sim 1 - e^{-\lambda_1}$$

$$A(-1) = B_1(0)B_2(0) \sim e^{-(\lambda_1+\lambda_2)}$$

$$\begin{aligned} \sum_{m=1}^{N_A-1} A(m)x^{m+1} &= \sum_{m=1}^{N_A-1} \sum_{m_1+m_2=m} B_1(m_1)B_2(m_2)x^{m+1} \\ &= \sum_{s=2}^{N_A} \sum_{r=0}^s B_1(s)B_2(s-r)x^s \\ &= \sum_{s=0}^{N_A} \sum_{r=0}^s B_1(s)B_2(s-r)x^s - B_1(0)B_2(0) - [B_1(0)B_2(1) + B_1(1)B_2(0)]x \\ &\rightarrow \left(\sum_{n=0}^{\infty} B_1(n)x^n \right) \left(\sum_{n=0}^{\infty} B_2(n)x^n \right) - B_1(0)B_2(0) - [B_1(0)B_2(1) + B_1(1)B_2(0)]x \quad (N_A \rightarrow \infty) \\ &= \exp[(\lambda_1 + \lambda_2)(x-1)] - e^{-(\lambda_1+\lambda_2)} [1 + (\lambda_1 + \lambda_2)x], \end{aligned}$$

where we have used the following identity of the generating function [20]: $\sum_{n \geq 0} \sum_{r=0}^n a_r b_{n-r} x^n = f \cdot g$, where $f = \sum_{n \geq 0} a_n x^n$ and $g = \sum_{n \geq 0} b_n x^n$. We thus obtain:

$$\begin{aligned} \frac{\partial Q}{\partial t} &= \eta Y(x) \frac{\partial Q}{\partial x} + Z(x)Q, \\ Y(x) &= \exp((\lambda_1 + \lambda_2)(x-1)) - x \exp(\lambda_1(x-1)), \\ Z(x) &= -1 + \exp(\lambda_1(x-1)). \end{aligned} \tag{A2}$$

In the stationary state, i.e. $\frac{\partial Q}{\partial t} \rightarrow 0$, we derive $Q'(1) \equiv \frac{\partial Q}{\partial x} \Big|_{x=1}$ and $Q''(1) = \frac{\partial^2 Q}{\partial x^2} \Big|_{x=1}$, and we obtain mean μ and variance σ^2 of the steady density distribution u_n^* . From the equation (A2),

$$\frac{Q'(x)}{Q(x)} = -\frac{Z(x)}{\eta Y(x)}.$$

In the limit of $x \rightarrow 1$, $\lim_{x \rightarrow 1} Y(x) = \lim_{x \rightarrow 1} Z(x) = 0$. Therefore:

$$\frac{Q'(1)}{Q(1)} = -\lim_{x \rightarrow 1} \frac{Z'(x)}{\eta Y'(x)}.$$

Using the normalized condition of $Q(1) = 1$:

$$Q'(1) = -\frac{Z'(1)}{\eta Y'(1)} = -\frac{N_A}{N} \kappa \cdot \frac{1}{\frac{N_A}{N} D \cdot (-\kappa)} = 1/D.$$

For $Q''(1)$, similarly we obtain:

$$Q''(1) = \frac{1}{2D\kappa} \left[1 - 2\kappa + \left(1 - \frac{N_A}{N} \right) \kappa^2 \right] + \frac{1}{D^2}.$$

Using $Q'(1)$ and $Q''(1)$, the mean μ and variance σ^2 of the steady density distribution u_n^* are given by [20],

$$\mu = Q'(1) = \frac{1}{D}$$

$$\sigma^2 = Q''(1) + Q'(1) - Q'(1)^2 = \frac{1}{2D\kappa} \left[1 - 2\kappa + \left(1 - \frac{N_A}{N} \right) \kappa^2 \right] + \frac{1}{D}.$$

The resource is given by $x = nD$, and then we finally obtain the mean μ_x and variance σ_x^2 of the resource distribution:

$$\mu_x = 1 \tag{A3}$$

$$\sigma_x^2 = \frac{D}{2\kappa} \left[1 - 2\kappa + \left(1 - \frac{N_A}{N} \right) \kappa^2 \right] + D. \tag{A4}$$